Computational aspects of the spectral Galerkin FEM for the Orr–Sommerfeld equation

N.P. Kirchner*

Technische Universität Darmstadt, Institut für Mechanik III, Hochschulstr. 1, D-64289 Darmstadt, Germany

SUMMARY

Since Orszag's paper ['Accurate solution of the Orr–Sommerfeld stability equation', *J. Fluid Mech.*, **50**, 689–703 (1971)], most of the subsequent spectral techniques for solving the Orr–Sommerfeld equation (OSE) employed the Tau discretization and Chebyshev polynomials. The use of the Tau discretization appears to be accompanied by so-called spurious eigenvalues not related to the OSE and a singular matrix B in the generalized eigenvalue problem. Starting from a variational formulation of the OSE, a spectral discretization is performed using a Galerkin method. By adopting integrated Legendre polynomials as basis functions, the boundary conditions can be satisfied exactly for any spectral order and the non-singular matrices A and B are obtained in $A\mathbf{x} = \lambda B\mathbf{x}$. For plane Poiseuille flow, the stiffness and the mass matrices are sparse with bandwidths 7 and 5 respectively, and the entries can be calculated explicitly (thus avoiding quadrature errors) for any polynomial flow profile U. According to the convergence results [Hancke, 'Calculating large spectra in hydrodynamic stability: a p FEM approach to solve the Orr–Sommerfeld equation', *Diploma Thesis*, Swiss Federal Institute of Technology Zürich, Seminar for Applied Mathematics, 1998; Hancke, Melenk and Schwab, 'A spectral Galerkin method for hydrodynamic stability problems', *Research Report No. 98-06*, Seminar for Applied Mathematics, Swiss Federal Institute of Technology, Zürich], no spurious eigenvalue has been found. Numerical experiments with spectral orders up to $p = 600$ illustrate the results. Copyright © 2000 John Wiley & Sons, Ltd.

KEY WORDS: hydrodynamic stability; sparse matrices; viscous shear flows

1. INTRODUCTION

The Orr–Sommerfeld equation, hereafter referred to as OSE, occurs in hydrodynamic stability theory [4]; it governs the stability of subsonic shear flows of viscous, Newtonian incompressible fluids, whose velocity field $\mathbf{u}$ satisfies rot $\mathbf{u} = \mathbf{0}$ (thus we have a potential flow). These flows may exist under various physical conditions, for instance, flows in a pipe or a channel, flows of superposed immiscible fluids, wakes, jets, plumes and free-streams in general. These flows

---

* Correspondence to: Technische Universität Darmstadt, Institut für Mechanik III, Hochschulstr. 1, D-64289 Darmstadt, Germany. E-mail: kirchner@mechanik.tu-darmstadt.de

may be laminar or turbulent and the transition from the former to the latter is essentially the above mentioned instability.
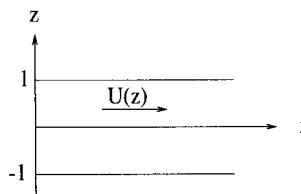
The general approach is to construct a laminar flow solution to the governing differential equations and boundary conditions and to superimpose the turbulent flow as small variations of the laminar flow. In the context of linearized modelling equations, the OSE is the equation from which a mathematical analysis of flow instabilities starts. The task is to determine the complex eigenvalues of the OSE, since the real part of the temporal growth rate of the disturbances is given by $e^{a\lambda_{imag}t}$ and amplified perturbations, i.e. those with $\lambda_{\mathrm{imag}} > 0$, become unbounded and make the flow unstable.

Early on, one is forced to employ numerical techniques in solving the OS eigenvalue problems: finite difference methods (FDM) were among the first by which the discretization of the OS eigenvalue equations were implemented. These turned out to be limited and more advanced techniques such as the finite element and spectral methods were proposed. Omitting any details, these techniques led to matrix eigenvalue problems with relatively fully occupied matrices. This unfortunate property essentially prevailed irrespective of whether the Galerkin, collocation or Tau method were used and limited the matrices to a certain size $K \times K$, with K being several hundreds in fortunate cases. Reliable results, however, can only be expected under the assumption of *scale resolution* [3], i.e. sufficiently small Re/p^2. Since in most cases of practical interest, the Reynolds number Re is large, $Re \geq \mathcal{O}(10^4)$, *high* spectral orders, $p \geq \mathcal{O}(10^3)$, have to be employed to obtain trustworthy results. (For Re_{crit}, which indicates the transition from laminar to turbulent flows, values of up to 40000 have been measured [5].) With fully occupied complex matrices, its computational corroboration is an impossible task. High spectral orders can only be implemented if the matrices are sparse and thus memory requirements are proportional to the spectral order.

In this paper, a method is proposed that generates sparsely occupied matrices and is therefore particularly suited to calculate large spectra at high accuracy.

1.1. Derivation of the OSE

We restrict our attention to the case of two-dimensional shear flows of an incompressible, viscous, Newtonian fluid flowing between two fixed, parallel plates. The dimensionless equations that govern the motion of the fluid are thus given by

$$\frac{\partial u}{\partial x} + \frac{\partial w}{\partial z} = 0, \tag{1}$$

$$\frac{\partial u}{\partial t} + u\frac{\partial u}{\partial x} + w\frac{\partial u}{\partial z} = -\frac{\partial p}{\partial x} + \frac{1}{Re}\left\{\frac{\partial^2 u}{\partial x^2} + \frac{\partial^2 u}{\partial z^2}\right\}, \tag{2}$$

$$\frac{\partial w}{\partial t} + u\frac{\partial w}{\partial x} + w\frac{\partial w}{\partial z} = -\frac{\partial p}{\partial z} + \frac{1}{Re}\left\{\frac{\partial^2 w}{\partial x^2} + \frac{\partial^2 w}{\partial z^2}\right\}. \tag{3}$$

To investigate the instability, we first construct a laminar steady solution $(\mathbf{U}, P)$ to Equations (1)–(3). Assuming the channel to be sufficiently 'long' (so that variations of the velocity field

in the streamwise direction may be neglected), an arbitrary two-dimensional, steady, incompressible flow field is given by $\mathbf{U} = (U(z), 0, 0)$, $P = P(x)$, where U can be at most quadratic in z for viscous flows [6].

The turbulent flow is now imposed on the basic flow $\mathbf{U}$, P as a small disturbance

$$\tilde{\mathbf{u}} = (\tilde{u}(x, z, t), 0, \tilde{w}(x, z, t)), \qquad \tilde{p} = \tilde{p}(x, z, t); \tag{4}$$

hence, we write

$$\mathbf{u} = \mathbf{U} + \varepsilon\tilde{\mathbf{u}}, \qquad p = P + \varepsilon\tilde{p}, \quad \text{with } 0 < \varepsilon \ll 1. \tag{5}$$

Since rot $\mathbf{u} = \mathbf{0}$, we can define the streamfunction $s = s(x, z, t)$ satisfying $u = \partial s/\partial z$, $w = -\partial s/\partial x$. We introduce a small disturbance $\tilde{s}(x, z, t) = \phi(z)\,\mathrm{e}^{\mathrm{i}a(x - ct)}$ to the streamfunction s, where ϕ is the amplitude function of $\tilde{s}$, a is a real wavenumber (if a were complex, spatial instabilities could occur in addition to the time-dependent ones) and c ($= \lambda = \lambda_\mathrm{R} + \mathrm{i}\lambda_\mathrm{I}$ in further applications) is the complex phase speed. Since the real part of the temporal growth rate of $\tilde{s}$ is $\mathrm{e}^{a\lambda_\mathrm{I}t}$, λ_I determines the stability of the disturbance: if $\lambda_\mathrm{I} < 0$, the amplitude of the disturbance decreases with time, hence the perturbation is stable. Letting $D = \partial/\partial z$, substitution of the disturbed flow into (1)–(3), neglecting terms of order higher than ε and forming the vorticity equation leads to

$$\mathrm{i}aRe(U - \lambda)(D^2 - a^2)\phi - \mathrm{i}aReD^2U\phi = (D^2 - a^2)^2\phi. \tag{6}$$

This is the Orr–Sommerfeld equation. For strictly parallel flows between fixed walls, Equation (6) is subjected to the boundary conditions

$$\phi = D\phi = 0, \qquad z = \pm 1. \tag{7}$$

Instability of two-dimensional laminar flow can now be discussed in terms of the eigenvalue problem (6) and (7).

1.2. Numerical approaches

To obtain a discrete version of (6), an approximate, ϕ_k, to the original solution may be written as a truncated series of appropriate basis functions N_i, i.e. $\phi_k = \Sigma_{i=1}^k a_i N_i$. Substitution of ϕ_k into (6) leads to a generalized matrix eigenvalue problem of the form $A\mathbf{x} = \lambda B\mathbf{x}$. Depending on the choice of basis functions, N_i, different discretization schemes are obtained: choosing infinitely differentiable global (with respect to the domain where the OSE is to be solved) basis functions N_i leads to the so-called *spectral methods*, whereas the choice of local basis functions is the typical feature of the *finite element methods* (FEM). Gottlieb and Orszag [7] give a compact review on the theory and application of spectral methods. Among the spectral methods, a further distinction depending on the choice of test functions is made: the three most commonly used discretization schemes are the Galerkin, collocation and Tau method.

In 1971, Orszag [1] used expansions in Chebyshev polynomials and a Tau method to transform the OSE into a matrix equation of the form $A\mathbf{x} = \lambda B\mathbf{x}$. Orszag discovered his results because of the special properties of the Chebyshev polynomials to be more accurate than those obtained previously. Almost all calculations were aimed at finding the least stable eigenvalue for plane Poiseuille flow and the critical Reynolds number. Ever since then, research has mainly followed the outlines given by Orszag. Unfortunately, it turned out that spurious eigenvalues (eigenvalues with large positive imaginary parts shifting wildly as the number of mesh points is increased) appear even in regimes where the flow is known to be stable [8,9]. Considerable effort has, therefore, been concentrated on developing methods that do not produce spurious eigenvalues. For instance, using separate expansions for the vorticity and streamfunction [7] eliminates the spurious modes, though at the expense that the matrices usually double in size.

McFadden *et al*. [10] pointed out that in solving $A\mathbf{x} = \lambda B\mathbf{x}$ resulting from the spectral–Tau approach, the matrix B is in general singular and that the occurrence of spurious modes is due to rows of zeros in B. Gardner *et al*. [9], McFadden *et al*. [10] and Lindsay and Ogden [11], to name a few, developed spectral methods resistant to the generation of spurious eigenvalues. Recently, Dongarra *et al*. [12] examined methods employing Chebyshev–Tau representations involving fourth, second and first derivative operators, respectively, and termed them the $D4$, $D2$ and D methods. In the case of the $D2$ and D method, the matrix B is inevitably singular owing to the way the boundary condition rows are added to A; A is relatively fully occupied, and the growth of the matrix coefficients is $\mathcal{O}(K^3)$ and $\mathcal{O}(K)$, where K is the spectral order. Only in the $D4$ method, is B non-singular, but a growth rate of $\mathcal{O}(K^7)$ of the matrix coefficients is likely to lead to round-off errors (especially since large values of K are required in actual calculations).

2. GALERKIN APPROACH

For the Galerkin approach, the OS eigenvalue problem in (6) and (7) is written in a variational formulation. The standard procedure [13] to cast Equations (6) and (7) in variational form is to multiply the equation with a so-called test function $\psi \in C_c^\infty(\Omega) = \{\psi \in C^\infty(\Omega): \text{supp } \psi \text{ is compact}\}$, and integrate it over the considered domain Ω, which in this case is the interval $(-1, 1)$. Let

$$L^2(-1, 1) := \left\{ \phi: (-1, 1) \to \mathbb{C}, \int_{-1}^{1} |\phi|^2 \, dz < \infty \right\}$$

be the space of complex-valued, square integrable functions on $(-1, 1)$ equipped with the scalar product

$$(\phi, \phi)_0 := \int_{-1}^{1} \phi(z) \overline{\phi(z)} \, dz.$$

We define the Sobolev space

$$H_0^2(-1, 1) := \{\phi \in L^2(-1, 1): D^\alpha \phi \in L^2(-1, 1), D^\alpha \phi(\pm 1) = 0, \alpha = 0, 1, 2\},$$

where D^α denotes the weak derivative. For convenience, the arguments of the functions as well as the domains of the function spaces will be dropped from now on. Multiplying (6) by $\bar{\psi} \in H_0^2$ and integration over Ω yields for the right-hand side

$$((D^2 - a^2)^2\phi, \psi)_0 = ((D^2 - a^2)\phi, \overline{(D^2 - a^2)\bar{\psi}})_0 = ((D^2 - a^2)\phi, (D^2 - a^2)\psi)_0,$$

where we have twice integrated by parts and used (7) to obtain the first equality, so that after rearranging terms we obtain the variational formulation of the OSE

$$((D^2 - a^2)\phi, (D^2 - a^2)\psi)_0 + Re(ia(D^2U)\phi, \psi)_0 - Re(ia((D^2 - a^2)\phi)U, \psi)_0$$
$$= -\lambda Re(ia(D^2 - a^2)\phi, \psi)_0 \quad \text{for all } \psi \in H_0^2. \tag{8}$$

We define bilinear forms

    a: $H_0^2 \times H_0^2 \to \mathbb{C}$, $\mathbf{a}(\phi, \psi) = $ left-hand-side of (8),
    b: $H_0^2 \times H_0^2 \to \mathbb{C}$, $\mathbf{b}(\phi, \psi) = -Re(ia(D^2 - a^2)\phi, \psi)_0,$

so that the OS eigenvalue problem is now given in the abstract variational form of

    Find $\phi \in H_0^2(-1, 1)$, $\lambda \in \mathbb{C}$ such that $\mathbf{a}(\phi, \psi) = \lambda \mathbf{b}(\phi, \psi)$ $\forall \psi \in H_0^2(-1, 1).$ (9)

Note that the boundary conditions are automatically satisfied. The existence of exact complex eigenvalues and corresponding (non-zero) eigenfunctions to (9) is well known (for details, see Hancke [2]).

2.1. Galerkin discretization

To treat (9) numerically, we have to restrict the problem to subspaces $V_K \subset H_0^2(-1, 1)$, which are finite-dimensional, $\dim V_K = K < \infty$. In this work, we will adhere to a simple mesh consisting of only one element $\Omega = (-1, 1)$ (which is identical with the so-called master element $\hat{\Omega} = (-1, 1)$, see Schwab [13]) and achieve convergence of our approximate solution by increasing the polynomial degree of the approximating functions (instead of refining the mesh).

Remark 2.1

To treat the flow of several superposed layers of different fluids, each of which has a profile $U(z)$, we choose the elements of the mesh according to the respective widths of the layers. Each element can then be mapped onto the master element, where the problem can be solved as proposed in this article. Finally, the solutions obtained on the master element can be mapped back to the respective element.

Definition 2.2
$V_K := \mathrm{span}\{N_i\}$, $i = 1, \ldots, p - 3$, where N_i are the so-called internal shape functions, defined by

$$N_i(z) := \sqrt{\frac{2i + 3}{2}} \int_{-1}^{z} \int_{-1}^{\eta} L_{i+1}(z) \, dz \, d\eta = \sqrt{\frac{2i + 3}{2}} \int_{-1}^{z} (z - \eta) L_{i+1}(\eta) \, d\eta, \tag{10}$$

where L_i is the ith Legendre polynomial.

A function $\phi_K \in V_K$ is therefore given by $\phi_K(z) = \Sigma_{i=1}^{K} \alpha_i N_i(z)$, with α_i being the scalar coefficients. The discrete version of (9) now reads

$$\text{Find} \quad \phi_K \in V_K, \ \lambda^{(K)} \in \mathbb{C} \quad \text{such that} \quad \mathbf{a}(\phi_K, \psi) = \lambda^{(K)} \mathbf{b}(\phi_K, \psi) \quad \forall \psi \in V_K. \tag{11}$$

Remark 2.3
Usually, the space V_K is spanned not only by internal but also by nodal shape functions (for details see Schwab [13]). In the present case, however, the boundary conditions imposed on the OSE, $\phi = D\phi = 0$, $z = \pm 1$, imply that the set of nodal shape functions is linearly dependent on the set of internal shape functions, thus accounting for dim $V_K = p - 3$.

Denoting $\partial/\partial z$ by a prime, we briefly state the following:

Proposition 2.4
The Legendre polynomials have the following properties [14]:

(a) $(2i + 1)L_i = L'_{i+1} - L'_{i-1}, \quad i = 1, 2, \ldots,$

(b) $(L_i, L_j)_0 = \int_{-1}^{1} L_i(z) L_j(z) \, dz = \begin{cases} \dfrac{2}{2i + 1}, & i = j \\ 0, & i \neq j \end{cases},$

(c) $L_i(-1) = (-1)^i, \qquad L_i(1) = 1,$

(d) $\int_{-1}^{z} L_{i+1}(\eta) \, d\eta = \dfrac{1}{2(i + 1) + 1} (L_{i+2}(z) - L_i(z)).$

We will frequently use the identities of

Corollary 2.5

(a) $N_i(z) = \sqrt{\dfrac{2i + 3}{2}} \left(\dfrac{L_{i+3}(z) - L_{i+1}(z)}{(2i + 3)(2i + 5)} - \dfrac{L_{i+1}(z) - L_{i-1}(z)}{(2i + 1)(2i + 3)} \right),$

(b) $DN_i(z) := \dfrac{\mathrm{d}}{\mathrm{d}z} N_i(z) = \dfrac{1}{\sqrt{2(2i+3)}} (L_{i+2}(z) - L_i(z))$,

(c) $D^2 N_i(z) = \sqrt{\dfrac{2i+3}{2}} L_{i+1}(z)$.

In all cases the results are obtained by straightforward calculation using integration by parts, Proposition 2.4 and the Leibniz rule.

3. STRUCTURE OF THE DISCRETE PROBLEM

We are now setting up the stiffness matrix A and the mass matrix B. As usual [13], $A_{ij} = \mathbf{a}(N_j, N_i)$ and $B_{ij} = \mathbf{b}(N_j, N_i)$. Due to the linearity and symmetry of the scalar product, we have

$$\begin{aligned}
\mathbf{a}(N_j, N_i) &= ((D^2 - a^2)N_j, (D^2 - a^2)N_i)_0 + Re(\mathrm{i}aN_j D^2 U, N_i)_0 - Re((D^2 - a^2)N_j U, \mathrm{i}aN_i)_0 \\
&= (D^2 N_j, D^2 N_i)_0 - 2a^2(D^2 N_j, N_i)_0 + a^4(N_j, N_i)_0 + Re\mathrm{i}a(N_j D^2 U, N_i)_0 \\
&\quad - Re\mathrm{i}a(UD^2 N_j, N_i)_0 + Re\mathrm{i}a^3(UN_j, N_i)_0 \\
&= T_{1ij} - 2a^2 T_{2ij} + a^4 T_{3ij} + Re\mathrm{i}a T_{4ij} - Re\mathrm{i}a T_{5ij} + Re\mathrm{i}a^3 T_{6ij},
\end{aligned} \tag{12}$$

where

$$\begin{array}{ll}
T_{1ij} := (D^2 N_j, D^2 N_i)_0, & T_{4ij} := (N_j D^2 U, N_i)_0, \\
T_{2ij} := (D^2 N_j, N_i)_0, & T_{5ij} := (UD^2 N_j, N_i)_0, \\
T_{3ij} := (N_j, N_i)_0, & T_{6ij} := (UN_j, N_i)_0.
\end{array}$$

Note that by integration by parts $(D^2 N_j, N_i)_0 = (N_j, D^2 N_i)_0$ holds, since $N_i, N_j \in V_K \subset H_0^2$; i.e. the functions and their derivative vanish at the boundary $z = \pm 1$. We will see that T_1, T_2, T_3 are banded due to the orthogonality of the Legendre polynomials. More precisely, T_1 is the identity, T_2 and T_3 have bandwidths 3 and 5 respectively, and the bands are not even fully occupied. Straightforward calculations show that every other diagonal consists of zero entries (again by orthogonality). Obviously, T_1, T_2 and T_3 are not affected by the mean flow $U(z)$, which for parallel shear flows of viscous fluids can be at most quadratic in z. The matrices T_4, T_5 and T_6, however, are affected by the mean flow, but nevertheless the band structure can be maintained [2], even for a general polynomial flow profile $U(z) = \Sigma_{i=0}^{k} a_i z^i$. Setting up the above matrices involves only basic mathematics: frequent use is made of the symmetry and linearity of the scalar product as well as of the properties of the Legendre polynomials stated in Section 2.

To calculate the matrices that are affected by the flow profile U, we need *Bonnet's recurrence formula* [15] for the Legendre polynomials

$$zL_k(z) = \frac{1}{2k+1}((k+1)L_{k+1}(z) + kL_{k-1}(z)) \quad \text{for } k = 1, 2, \ldots \tag{13}$$

For plane Poiseuille flow, i.e. $U(z) = 1 - z^2$, we immediately obtain $T_4 = -2T_3$, $T_5 = T_2 - T_5^*$, with $T_{5ij}^* := (z^2 D^2 N_j, N_i)_0$ and $T_6 = T_3 - T_6^*$, with $T_{6ij}^* := -(z^2 N_j, N_i)_0 = T_{3ij} - T_{6ij}^*$. The explicit calculations for any matrix entry of A can be found in detail in Appendix B; setting up the mass matrix B proceeds along the same lines.

According to (12), we have to equip the matrices T_i with multiplicative factors involving the Reynolds number Re and the wavelength a to set up the stiffness matrix A and arrive at

$$A = T_1 - (2a^2 + Re\mathrm{i}a)T_2 + (a^4 - 2Re\mathrm{i}a + Re\mathrm{i}a^3)T_3 + Re\mathrm{i}aT_5^* - Re\mathrm{i}a^3T_6^*, \tag{14}$$

where terms have been collected. Similarly, we obtain for the mass matrix B,

$$B = -Re\mathrm{i}aT_2 + Re\mathrm{i}aT_3. \tag{15}$$

As shown in the appendix, we therefore conclude

For plane Poisenille flow, the stiffness matrix $A \in \mathcal{M}(p - 3, p - 3)$ and the mass matrix $B \in \mathcal{M}(p - 3, p - 3)$ have bandwidths 7 and 5 respectively, no matter how large the value of p is. All entries A_{ij}, B_{ij} can be computed explicitly, thereby avoiding quadrature errors. Such sparse matrices are particularly suited to the calculation of large spectra in hydrodynamic stability, since memory requirements are proportional to the spectral order and high spectral orders are necessary to guarantee scale resolution and therefore trustworthy results.

4. NUMERICAL RESULTS

In this section we present the numerical eigenvalue approximations obtained with the p-FEM approach. First, the spectrum of plane Poiseuille flow at a Reynolds number $Re = 10^4$, which has been studied by several authors [1,12,16], is addressed. Next, we examine the critical values of λ and Re for the classical problem of plane Poiseuille flow and compare our results in detail with those of previous investigations based on the Chebychev–Tau spectral approach, in particular with Orszag [1] and Dongarra *et al.* [12].

We demonstrate p-convergence of the eigenvalues emerging from the discretized problem to the exact eigenvalues. Then, we turn to higher Reynolds numbers of order 10^5 and above. Here the conditioning of the discrete problem is essential and therefore investigated. It appears that the least stable modes can reliably be approximated by the p-FEM approach provided the polynomial degree is suitably increased with Re. Trustworthy results can only be obtained under the assumption of *scale resolution* [3], i.e. small Re/p^2.

All calculations are performed for plane Poiseuille flow and are based on 64-bit arithmetic using standard eigenvalue software (MATLAB V).

4.1. Numerical solution

We have to solve the generalized eigenvalue problem $A\mathbf{x} = \lambda B\mathbf{x}$, where $A, B \in \mathcal{M}(K, K)$ have been computed explicitly in the preceding section (respectively in the appendix), $\mathbf{x} \in \mathbb{R}^K$ and $\lambda \in \mathbb{C}$. The eigenvalues λ can, for example, be found by using the QZ algorithm, which we shall now briefly describe.

Given $A, B \in \mathcal{M}(K, K)$, the QZ algorithm computes matrices $Q, Z \in \text{orth}(K, K)$ such that $Q^T A Z = T$ is upper (quasi-)triangular with diagonal elements t_{ii}, and $Q^T B Z = S$ is upper triangular with diagonal elements s_{ii}. The eigenvalues of $A\mathbf{x} = \lambda B\mathbf{x}$ are then given by $\lambda_i = t_{ii}/s_{ii}$, for $i = 1, \ldots, K$, where division makes sense. The algorithm requires roughly $30K^3$ flops. For details, see Golub and van Loan [17]. It should be noted that the QZ algorithm can be applied to any two square (complex) matrices.

We wrote a MATLAB code that generates the matrices A and B for any prescribed polynomial degree p given the physical setting of plane Poiseuille flow. Using the QZ algorithm implemented in the MATLAB V version, we were not able to exploit the sparsity of the matrices, since full matrices are required as input data. In principle, however, the sparsity of the matrices opens the way to the use of large spectral orders.

4.2. The spectrum for plane Poiseuille flow at $Re = 10^4$

The spectrum for plane Poiseuille flow, $p = 500$, $Re = 10^4$ and $a = 1$ obtained from the p-FEM is shown in Figure 1. We restricted the display to those eigenvalues with $\lambda_I \geq -1$, which is common in fluid dynamics; the disturbances corresponding to eigenvalues with large negative imaginary parts are of little practical interest since they decay quickly in time.

Focusing on the least stable modes (i.e. those with largest imaginary parts), we investigated possible inaccuracies resulting from the growing size of the problem and compared the spectra obtained with $p = 200$ and $p = 500$ for the plane Poiseuille flow. They are shown in Figure 2(a)
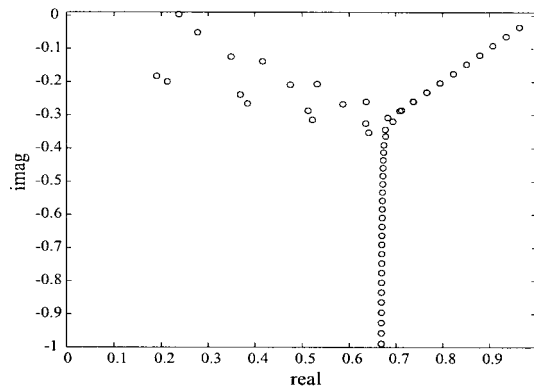

Figure 1. Spectrum for plane Poiseuille flow at $Re = 10^4$, $a = 1$, $p = 500$.

and (b). Irrespective of p no changes of position in the branches could be detected. Only a slight shifting of positions occurs around the branching point, but this region is known to be very sensitive to changes in Re and p, as reported by e.g. Orszag [1] and Dongarra *et al.* [12]. We conclude that we do not have to cope with major numerical inaccuracies caused by the growing size of the problem as far as the least stable modes at a moderate Reynolds number are concerned.

4.3. The critical values of λ and Re for plane Poiseuille flow

To put the p-FEM for the OSE to a first test, we calculated the critical Reynolds number Re_{crit} (given $a = 1.026$) and the critical eigenvalue λ_{crit} for plane Poiseuille flow (at $Re = 10^4$, $a = 1$). The results are presented in Tables I and II.

Concerning Table II, we remark that Orszag used only even modes in his calculation of λ_{crit} and that with the $D4$ method, Dongarra *et al.* solve $A\mathbf{x} = \lambda B\mathbf{x}$ with a non-singular B and a relatively fully occupied A. Two spurious modes occur, questioning the belief that such modes are related only to a singular B, but rather to the Tau discertization technique. Moreover, the values obtained for λ_{crit} diverge from ($*$) with increasing spectral order K.
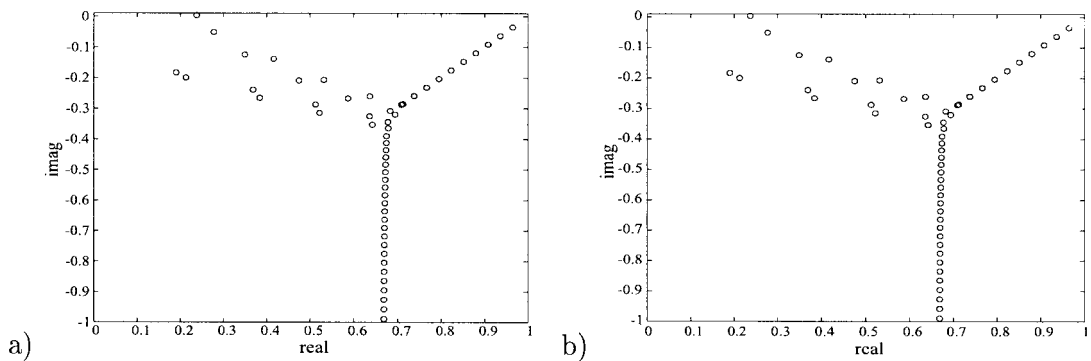

Figure 2. Spectrum for plane Poiseuille flow at $Re = 10^4$, $a = 1$, $p = 200$ (a) and $p = 500$ (b).

Table I. Re_{crit} for plane Poiseuille flow

	Wavenumber a	Re_{crit}
Thomas	1.026	5780
Orszag	1.02056 ± 0.00001	5772.22
Nachtsheim[a]	1.02	5767
Grosch and Salwen[a]	1.025	5750
Present work	1.026	5775.99

[a] Results reported by Orszag [1].

Table II. Least stable mode for plane Poiseuille flow

λ_{crit}		Method
Thomas		FDM
0.2375006	$+0.0035925i$	50 Grid points
0.2375243	$+0.0037312i$	100 Grid points
Orszag		Chebyshev–Tau
0.23752649	$+0.00373967i$ (*)	$K = 28$
Dongarra et $al.$		$D4$ method
0.23752708	$+0.00373980i$	$K = 50$
Present work		p-FEM
$2.375264900288206e-01$	$+3.739669595990969e-03i$	$p = 50$
$2.375264888204705e-01$	$+3.739670622980277e-03i$	$p = 100$
$2.375264888204710e-01$	$+3.739670622980398e-03i$	$p = 200$
$2.375264888204704e-01$	$+3.739670622979626e-03i$	$p = 300$
$2.375264888204682e-01$	$+3.739670622979878e-03i$	$p = 400$
$2.375264888204705e-01$	$+3.739670622979582e-03i$	$p = 500$

4.4. Least stable mode for plane Poiseuille flow

Orszag [1] lists the 32 least stable modes obtained with the Spectral–Tau method and a spectral order $K \leq 100$. With the p-FEM, excellent agreement on all 32 modes is achieved. We have not found a single spurious mode. Dongarra et $al.$ [12] found an extra eigenvalue between positions 17 and 18 of Orszag's list; the p-FEM confirmed this result. The list of the least 33 stable eigenvalues is given in Appendix A. We now demonstrate the p-convergence behaviour of the least stable mode for plane Poiseuille flow at $a = 1$, $Re = 10^4$ (Table III). The corresponding eigenfunction, whose regularity strongly influences the convergence of the eigenvalue, is shown in Figure 3. This plot supports our statement that the eigenvalue is converged. For a detailed convergence analysis of the five least stable modes see Hancke [2].

4.5. Least stable modes at $Re = 10^5$ to $Re = 10^9$

Since for large Reynolds number only few data are available to compare our results with, we will restrict our attention to results concerning the least stable mode, for which at least some calculations have been performed. We will compare our results with the ones obtained by Dongarra et $al.$ [12] and Abdullah and Lindsay [18].

Table III. Convergence of the least stable mode

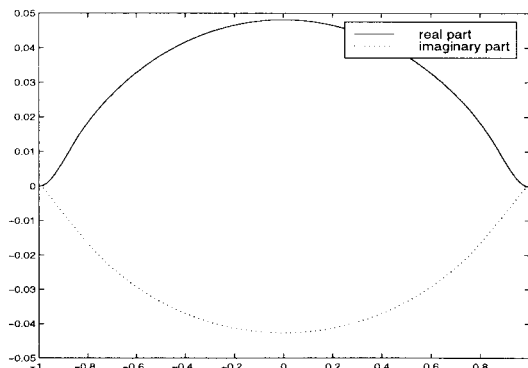| $p = 100$	$2.375264888204705e-01 + 3.739670622980277e-03i$
$p = 200$	$2.375264888204710e-01 + 3.739670622980398e-03i$
$p = 300$	$2.375264888204704e-01 + 3.739670622979626e-03i$
$p = 400$	$2.375264888204682e-01 + 3.739670622979878e-03i$
$p = 500$	$2.375264888204682e-01 + 3.739670622979878e-03i$

Figure 3. Eigenfunction to the least stable mode.

For Reynolds numbers larger than $Re = 10^5$, we tested our code against the results obtained by Abdullah and Lindsay [18]. Table IV gives the numerical results for the imaginary part of the critical, least stable eigenvalue for plane Poiseuille flow and $a = 1$. Only the significant figures are shown. The polynomial degree is kept fixed at $p = 600$. Note that this table is not to be understood in the sense that plane Poiseuille flow is stable at such high Reynolds numbers: for large values of Re the transition from laminar flow to turbulent flow is shifted to higher wavenumbers than $a = 1$. Unfortunately, no experimental data on Reynolds number/ wavenumber combinations that yield the expected unstable disturbances were available to us to put the p-FEM code to a further test.

For plane Poiseuille flow, $a = 1$ and $Re = 10^5$, Dongarra *et al*. present the eigenvalues with the largest imaginary parts for the six odd and even eigenfunctions obtained from the $D2$ method using 400 polynomials (Table V). We performed respective calculations and present Table VI for comparison, where we limited the display to the significant figures.

Table IV. Least stable mode at various Reynolds numbers, obtained by Abdullah and Lindsay [18], and with the p-FEM

Re	Abdullah and Lindsay	Present work	p
10^4	$+0.003739i$	$+0.00373967i$	600
10^5	$-0.011164i$	$-0.01116257i$	600
10^6	$-0.003534i$	$-0.00353380i$	600
10^7	$-0.001118i$	$-0.00111786i$	600
10^8	$-0.000354i$	$-0.00035353i$	600
10^9	$-0.000112i$	$-0.00012091i$	600

Table V. Least stable modes at $Re = 10^5$, $a = 1$ obtained by Dongarra *et al.* [12]

Odd	$9.888191058e - 01 - 1.116257893e - 02i$
	$9.798738045e - 01 - 2.008374163e - 02i$
	$9.709280339e - 01 - 2.900433538e - 02i$
	$1.373944878e - 01 - 2.956356969e - 02i$
	$9.619817790e - 01 - 3.792441466e - 02i$
	$9.530350180e - 01 - 4.684401422e - 02i$
Even	$9.888195933e - 01 - 1.116360699e - 02i$
	$1.459247829e - 01 - 1.504203085e - 02i$
	$9.798751271e - 01 - 2.008635538e - 02i$
	$9.709305305e - 01 - 2.900898101e - 02i$
	$1.982003566e - 01 - 3.733100660e - 02i$
	$9.619857994e - 01 - 3.793148490e - 02i$

Table VI. Least stable modes at $Re = 10^5$, $a = 1$ obtained with the p-FEM

Odd	$9.888191058e - 01 - 1.116257892e - 02i$
	$9.798738045e - 01 - 2.008374162e - 02i$
	$9.709280338e - 01 - 2.900433537e - 02i$
	$1.373944863e - 01 - 2.956360012e - 02i$
	$9.619817790e - 01 - 3.792441474e - 02i$
	$9.530350177e - 01 - 4.684401411e - 02i$
Even	$9.888195933e - 01 - 1.116360699e - 02i$
	$1.459247885e - 01 - 1.504204266e - 02i$
	$9.798751270e - 01 - 2.008635541e - 02i$
	$9.709305303e - 01 - 2.900898109e - 02i$
	$1.982003544e - 01 - 3.733101358e - 02i$
	$9.619857991e - 01 - 3.793148468e - 02i$

The results presented in this section show clearly that the p-FEM approach is a viable alternative to the existing spectral methods commonly used to tackle hydrodynamic instability problems.

4.6. Condition of A and B

The conditioning of the discrete problem becomes essential if a high polynomial degree p is required to achieve convergence. Numerically, the conditioning of A and B has been investigated by performing calculations with up to $p = 500$ for various prescribed Reynolds numbers using MATLAB V. A theoretical analysis of the upper bounds of the condition of A and B can be found in Hancke [2]. For the definition of the condition of a matrix we refer to Golub and van Loan [17]. Figure 4(a) shows that the condition number of A, cond(A), remains at a constant value in all considered cases if calculated for a 'sufficiently large' p, which for Reynolds numbers up to 270000 was found to be $p = 100$. From this we derive that the condition of A depends linearly on the Reynolds number if $p \geqslant 100$. Figure 4(b) plots the
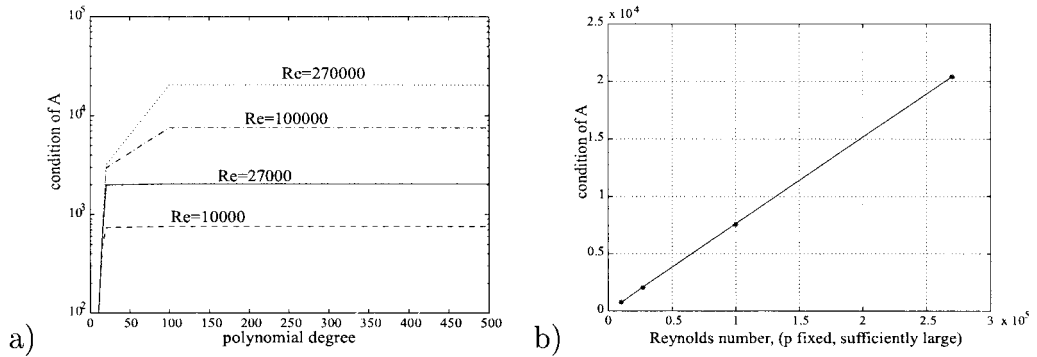
Figure 4. cond(A) as a funciton of the spectral order p for various Reynolds numbers (a) and cond(A) as a function of the Reynolds number (b).

condition of A as a function of Re for $p = 500$. The condition of B is found to be independent of the Reynolds number: theoretical investigations [2] imply that cond(B) $\leq Cp^4$, where $C = 40$ has been found from numerical experiments. From this, we see that it is necessary to use higher precision if p becomes large.

5. CONCLUSION

In the present work, we proposed a spectral discretization using a Galerkin method starting form a variational formulation of the OSE. We adopted integrated Legendre polynomials as basis functions and wrote a MATAB code that generates the sparse matrices A and B for any prescribed polynomial of degree p, where p is the spectral order. The boundary conditions imposed for strictly parallel flow between fixed plates are satisfied exactly for any p by the specific choice of the shape functions. Due to the orthogonality property of the Legendre polynomials on the interval $(-1, 1)$, sparse matrices are obtained of which the entries are explicitly computable. Memory requirements are thus proportional to p and quadrature errors are avoided. For the plane Poiseuille flow profile $U(z) = 1 - z^2$, the matrices A and B have a bandwidth of 7 and 5 respectively, independent of p. The matrices are non-singular and relatively well conditioned. We found no spurious eigenvalues. The numerical results existing for the plane Poiseuille flow profile at various Reynolds numbers were duplicated in all cases, while all calculations were performed by using standard eigenvalue software (MATLAB V) and based on 64-bit arithmetic. Using MATLAB V, we could not exploit the sparsity of the matrices since the QZ algorithm in MATLAB requires *full* matrices as input data. To take advantage of the sparsity of A and B, Arnoldi or unsymmetric Lanczos methods (see Golub and van Loan [17] and the references therein) should be employed in the future.

APPENDIX A. LEAST STABLE MODES FOR PLANE POISEUILLE FLOW

Table VII lists the 33 least stable modes for plane Poiseuille flow at $Re = 10^4$, $a = 1$. Between position 17 and 18 of Orszag's list, we confirmed the occurrence of an extra eigenvalue—now position 18—as reported recently by Dongarra *et al.* [12].

Table VII. The 33 least stable modes determined by the p-FEM for plane Poiseuille flow, $a = 1$, $Re = 10^4$, $p = 500$

1	$2.375264888204705e-01+3.739670622979582e-03i$
2	$9.646309154506005e-01-3.516727763102714e-02i$
3	$9.646425100392918e-01-3.518658379244360e-02i$
4	$2.772043438088034e-01-5.089872725696934e-02i$
5	$9.363165358813165e-01-6.320149583992261e-02i$
6	$9.363517811647321e-01-6.325156907426489e-02i$
7	$9.079830546294746e-01-9.122273543365587e-02i$
8	$9.080563344920409e-01-9.131286177906131e-02i$
9	$8.796272922071848e-01-1.192328526196531e-01i$
10	$8.797556958148425e-01-1.193707310084970e-01i$
11	$3.491068201236155e-01-1.245019775533640e-01i$
12	$4.163510155757767e-01-1.382265253008422e-01i$
13	$8.512458401250318e-01-1.472339290761887e-01i$
14	$8.514493818788961e-01-1.474256007529050e-01i$
15	$8.228350406919021e-01-1.752286786585769e-01i$
16	$8.231369612637365e-01-1.754780735545809e-01i$
17	$1.900592493682396e-01-1.828219254122324e-01i$
18	$2.127257823532061e-01-1.993606947537152e-01i$
19	$7.943883849501244e-01-2.032206650325090e-01i$
20	$7.948183878533778e-01-2.035291440331918e-01i$
21	$5.320452087705384e-01-2.064652191027814e-01i$
22	$4.749011869505417e-01-2.087312200483873e-01i$
23	$7.658768104861932e-01-2.311859867400237e-01i$
24	$7.664940761566144e-01-2.315850738517848e-01i$
25	$3.684984783489053e-01-2.388248317189281e-01i$
26	$7.374157633012601e-01-2.587170766094873e-01i$
27	$7.381150139815603e-01-2.596918833434765e-01i$
28	$6.367193722661181e-01-2.598857149326573e-01i$
29	$3.839876109046220e-01-2.651064996075110e-01i$
30	$5.872129330137613e-01-2.671617095172383e-01i$
31	$7.123158607293292e-01-2.855147340989841e-01i$
32	$5.129162044954282e-01-2.866250415845459e-01i$
33	$7.088746522936619e-01-2.876553939185146e-01i$

APPENDIX B. CALCULATION OF THE MATRIX ENTRIES A_{ij}

B.1. Calculation of $T_{1ij} := (D^2 N_j, D^2 N_i)_0$ for $1 \leq i, j \leq p - 3$

By Corollary 2.5 and the orthogonality we have

$$(D^2 N_j, D^2 N_i)_0 = \frac{\sqrt{2j+3}\sqrt{2i+3}}{2} \frac{2}{2j+3} \delta_{ij} = \begin{cases} 1, & i = j \\ 0, & i \neq j \end{cases},$$

thus T_1 is the identity matrix.

B.2. Calculation of $T_{2ij} := (D^2 N_j, N_i)_0$ for $1 \leq i, j \leq p - 3$

Using Proposition 2.4 and Corollary 2.5, we obtain for the non-zero entries

$$T_{2ij}^* = \begin{cases} i = j - 2: & \dfrac{1}{\sqrt{2j-1}(2j+1)\sqrt{2j+3}}, \\[2ex] i = j: & -\dfrac{1}{2j+3}\left(\dfrac{1}{2j+1} + \dfrac{1}{2j+5}\right), \\[2ex] i = j + 2: & \dfrac{1}{\sqrt{2j+3}(2j+5)\sqrt{2j+7}}, \end{cases}$$

since

$$(D^2 N_j, N_i)_0 = \frac{\sqrt{2j+3}\sqrt{2i+3}}{2} \int_{-1}^{1} \left(\frac{L_{j+1}(L_{i+3} - L_{i+1})}{(2i+3)(2i+5)} - \frac{L_{j+1}(L_{i+1} - L_{i-1})}{(2i+1)(2i+3)} \right) \mathrm{d}z.$$

B.3. Calculation of $T_{3ij} := (N_j, N_i)_0$ for $1 \leq i, j \leq p - 3$

Calculations do not differ from the ones carried out for T_1, T_2. Since T_3 is symmetric, we will only display the diagonal and upper diagonal (non-zero) entries. We have

$$(N_j, N_i)_0 = \sqrt{\frac{2j+3}{2}} \sqrt{\frac{2i+3}{2}} \int_{-1}^{1} IJ \, \mathrm{d}z,$$

where $I := \int_{-1}^{z} (z - \eta) L_{i+1}(\eta) \, \mathrm{d}\eta$ and $J := \int_{-1}^{z} (z - \eta) L_{j+1}(\eta) \, \mathrm{d}\eta$. Obviously,

$$\int_{-1}^{1} IJ \, \mathrm{d}z = \int_{-1}^{1} I_1 J_1 \, \mathrm{d}z - \int_{-1}^{1} I_1 J_2 \, \mathrm{d}z - \int_{-1}^{1} I_2 J_1 \, \mathrm{d}z + \int_{-1}^{1} I_2 J_2 \, \mathrm{d}z, \tag{16}$$

where

$$I_1(z) = \frac{L_{i+3}(z) - L_{i+1}(z)}{(2i+3)(2i+5)}, \quad I_2(z) = \frac{L_{i+1}(z) - L_{i-1}(z)}{(2i+1)(2i+3)},$$

$$J_1(z) = \frac{L_{j+3}(z) - L_{j+1}(z)}{(2j+3)(2j+5)}, \quad J_2(z) = \frac{L_{j+1}(z) - L_{j-1}(z)}{(2j+1)(2j+3)}.$$

By Proposition 2.4(b), each integral on the right-hand side of (16) can be simplified considerably by straightforward calculations. Putting the various pieces together and finally multiplying with the so far omitted factor $(\sqrt{2i+3}\sqrt{2j+3})/2$ yields for the diagonal and upper diagonal entries

$$T_{3ij} = \begin{cases} i = j - 4: & \dfrac{1}{\sqrt{2j-5}(2j-3)(2j-1)(2j+1)\sqrt{2j+3}}, \\[2mm] i = j - 2: & \dfrac{-1}{\sqrt{2j-1}(2j+1)\sqrt{2j+3}} \\[2mm] & \left(\dfrac{1}{(2j+3)(2j+5)} + \dfrac{1}{(2j+1)(2j+3)} + \dfrac{1}{(2j-1)(2j+1)} + \dfrac{1}{(2j-1)(2j-3)} \right), \\[3mm] i = j: & \dfrac{1}{2j+3} \left(\dfrac{1}{(2j+5)^2(2j+7)} + \dfrac{1}{(2j+3)(2j+5)^2} \right. \\[3mm] & \left. + \dfrac{2}{(2j+1)(2j+3)(2j+5)} + \dfrac{1}{(2j+1)^2(2j+3)} + \dfrac{1}{(2j+1)^2(2j-1)} \right). \end{cases}$$

B.4. Calculation of $T_{4ij} := (N_j D^2 U, N_i)_0$ for $1 \le i, j \le p - 3$

For plane Poiseuille flow, where $U(z) = 1 - z^2$, we obtain $T_4 = -2T_3$.

B.5. Calculation of $T_{5ij} := (U D^2 N_j, N_i)_0$ for $1 \le i, j \le p - 3$

Note that $(z^2 L_j, L_k)_0 = (zL_j, zL_k)_0$ holds because of the symmetry of the scalar product and since z is real. Thus, we can evaluate these expressions using Bonnet's formula. For $U(z) = 1 - z^2$ we arrive at $(U D^2 N_j, N_i)_0 = (D^2 N_j, N_i)_0 - (z^2 D^2 N_j, N_i)_0 = T_{2ij} - T^*_{5ij}$, so that T_5 is composed of the already computed matrix T_2 and the matrix T^*_5 defined in Section 3. It should be mentioned that T^*_5 is not symmetric. We present merely the results

$$T^*_{5ij} = \begin{cases} i = j - 4: & \dfrac{j(j+1)}{\sqrt{2j-5}(2j-3)(2j-1)(2j+1)\sqrt{2j+3}}, \\[2mm] i = j - 2: & \dfrac{1}{\sqrt{2j-1}(2j+1)\sqrt{2j+3}} \left(\dfrac{(j+2)^2}{(2j+3)(2j+5)} \right. \\[3mm] & \left. + \dfrac{(j+1)^2}{(2j+1)(2j+3)} - \dfrac{j(j+1)}{(2j-1)(2j+1)} - \dfrac{j(j+1)}{(2j-3)(2j-1)} \right), \\[3mm] i = j: & \dfrac{1}{2j+3} \left(\dfrac{(j+2)(j+3)}{(2j+5)^2(2j+7)} - \dfrac{(j+2)^2}{(2j+3)(2j+5)^2} \right. \\[3mm] & - \dfrac{(j+1)^2}{(2j+1)(2j+3)(2j+5)} - \dfrac{(j+2)^2}{(2j+1)(2j+3)(2j+5)} + \dfrac{j(j+1)}{(2j+1)^2(2j-1)} \\[3mm] & \left. - \dfrac{(j+1)^2}{(2j+1)^2(2j+3)} \right), \\[3mm] i = j + 2: & \dfrac{1}{\sqrt{2j+3}(2j+5)\sqrt{2j+7}} \left(\dfrac{(j+4)^2}{(2j+7)(2j+9)} \right. \\[3mm] & \left. + \dfrac{(j+3)^2}{(2j+5)(2j+7)} - \dfrac{(j+2)(j+3)}{(2j+3)(2j+5)} - \dfrac{(j+2)(j+3)}{(2j+1)(2j+3)} \right), \\[3mm] i = j + 4: & \dfrac{(j+2)(j+3)}{\sqrt{2j+3}(2j+5)(2j+7)(2j+9)\sqrt{2j+11}}. \end{cases}$$

B.6. Calculation of $T_{6ij} := (UN_j, N_i)_0$ for $1 \leq i, j \leq p - 3$

For plane Poiseuille flow, $T_{6ij} = (N_j, N_i)_0 - (z^2 N_j, N_i)_0 = T_{3ij} - T^*_{6ij}$, where T^*_6 is a symmetric matrix whose diagonal and upper diagonal nonzero entries are given by

$$T^*_{6ij} =$$

$i = j - 6$:
$$\frac{(j-2)(j-1)}{\sqrt{2j-9}(2j-7)(2j-5)(2j-3)(2j-1)(2j+1)\sqrt{2j+3}},$$

$i = j - 4$:
$$\frac{1}{\sqrt{2j-5}(2j-3)(2j-1)(2j+1)\sqrt{2j+3}} \left(-\frac{j(j+1)}{(2j+3)(2j+5)} - \frac{j(j+1)}{(2j+1)(2j+3)} \right.$$
$$\left. + \frac{j^2}{(2j-1)(2j+1)} + \frac{(j-1)^2}{(2j-3)(2j-1)} - \frac{(j-2)(j-1)}{(2j-5)(2j-3)} - \frac{(j-2)(j-1)}{(2j-7)(2j-5)} \right),$$

$i = j - 2$:
$$\frac{1}{\sqrt{2j-1}(2j+1)\sqrt{2j+3}} \left(\frac{(j+2)(j+3)}{(2j+3)(2j+5)^2(2j+7)} - \frac{(j+2)^2}{(2j+3)^2(2j+5)^2} \right.$$
$$- \frac{j^2}{(2j-1)^2(2j+1)^2} - \frac{(j+1)^2}{(2j+1)^2(2j+3)^2} - \frac{(j+2)^2}{(2j+1)(2j+3)^2(2j+5)}$$
$$+ \frac{2(j+1)j}{(2j-1)(2j+1)^2(2j+3)} + \frac{j(j+1)}{(2j-1)(2j+1)(2j+3)(2j+5)}$$
$$- \frac{(j+1)^2}{(2j+1)(2j+3)^2(2j+5)} - \frac{(j-1)^2}{(2j-3)(2j-1)^2(2j+1)}$$
$$+ \frac{j(j+1)}{(2j-3)(2j-1)(2j+3)(2j+5)} + \frac{j(j+1)}{(2j-3)(2j-1)(2j+3)(2j+1)}$$
$$\left. - \frac{j^2}{(2j-3)(2j-1)^2(2j+1)} - \frac{(j-1)^2}{(2j-1)^2(2j+1)^2} + \frac{(j-2)(j-1)}{(2j-5)(2j-3)^2(2j-1)} \right),$$

$i = j$:
$$\frac{1}{2j+3} \left(\frac{(j+4)^2}{(2j+5)^2(2j+7)^2(2j+9)} + \frac{(j+3)^2}{(2j+5)^3(2j+7)^2} - \frac{2(j+3)(j+2)}{(2j+3)(2j+5)^3(2j+7)} \right.$$
$$- \frac{2(j+3)(j+2)}{(2j+1)(2j+3)(2j+5)^2(2j+7)} + \frac{(j+2)^2}{(2j+3)^2(2j+5)^3} + \frac{(j+1)^2}{(2j+1)(2j+3)^2(2j+5)^2}$$
$$+ \frac{2(j+2)^2}{(2j+1)(2j+3)^2(2j+5)^2} + \frac{2(j+1)^2}{(2j+1)^2(2j+3)^2(2j+5)^2} - \frac{2j(j+1)}{(2j-1)(2j+1)^2(2j+3)(2j+5)}$$
$$+ \frac{(j+2)^2}{(2j+1)^2(2j+3)^2(2j+5)} + \frac{(j+1)^2}{(2j+1)^3(2j+3)^2} - \frac{2j(j+1)}{(2j-1)(2j+1)^3(2j+3)}$$
$$\left. + \frac{j^2}{(2j-1)(2j+1)^3} + \frac{(j-1)^2}{(2j-3)(2j-1)^2(2j+1)^2} \right).$$

REFERENCES

1. S.A. Orszag, ;Accurate solution of the Orr–Sommerfeld stability equation', *J. Fluid Mech.*, **50**, 689–703 (1971).
2. N.P. Hancke, 'Calculating large spectra in hydrodynamic stability: a *p*-FEM approach to solve the Orr–Sommerfeld equation', *Diploma Thesis*, Seminar for Applied Mathematics, Swiss Federal Institute of Technology Zürich, 1998.
3. N.P. Hancke, J.M. Melenk and C. Schwab, 'A spectral Galerkin method for hydrodynamic stability problems', *Research Report No. 98-06*, Seminar for Applied Mathematics, Swiss Federal Institute of Technology Zürich, 1998.
4. P.G. Drazin and W.H. Reid, *Hydrodynamic Stability*, Cambridge University Press, Cambridge, 1981.
5. J.H. Spurk, *Strömungslehre*, 2nd edn, Springer, Berlin, 1989.
6. K. Hutter, *Fluid- und Thermodynamik*, Springer, Berlin, 1995.
7. D. Gottlieb and S.A. Orszag, *Numerical Aspects of Spectral Methods: Theory and Applications*, SIAM-CB\IS, Philadelphia, 1972.
8. J. Gary and R. Helgason, 'A matrix method for ordinary differential eigenvalue problems', *J. Comput. Phys.*, **5**, 169–187 (1970).
9. D.R. Gardner, S.A. Trogden and R.W. Douglass, 'A modified Tau spectral method that eliminates spurious eigenvalues', *J. Comput. Phys.*, **80**, 169–187 (1970).
10. G.B. McFadden, B.T. Murray and R.F. Boisvert, 'Elimination of spurious eigenvalues in the Chebyshev Tau spectral method', *J. Comput. Phys.*, **91**, 228–239 (1990).
11. K.A. Lindsay and R.R. Ogden, 'A practical implementation of spectral methods resistant to the generation of spurious eigenvalues', *Int. J. Numer. Methods Fluids*, **15**, 1277–1294 (1992).
12. J.J. Dongarra, B. Straughan and D.W. Walker, 'Chebyshev Tau–QZ algorithm methods for calculating spectra of hydrodynamic stability problems', *Appl. Numer. Math.*, **22**, 399–434 (1996).
13. C. Schwab, *p- and hp-Finite Element Methods*, Oxford University Press, Oxford, 1998.
14. M. Abramowitz and I.A. Stegun, *Handbook of Mathematical Functions*, Dover, New York, 1971.
15. H.R. Schwarz, *Numerische Mathematik*, 2nd edn, Teubner, Stuttgart, 1988.
16. L.H. Thomas, 'The stability of plane Poiseuille flow', *Phys. Rev.*, **91**, 780–783 (1953).
17. G.H. Golub and C.F. van Loan, *Matrix Computation*, The Johns Hopkins University Press, Baltimore, MD, 1996.
18. A.A. Abdullah and K.A Lindsay, 'Some remarks on computation of eigenvalues of linear systems', *Math. Models Methods Appl. Sci.*, **1**, 153–165 (1991).